Non invasive and real time analysis of skin pigmentation and cutaneous hemoglobin oxygenation: An experimental and theoretical approach.

Eleni Drakaki,[1]
1. Physics Department, National Technical University of Athens,
Zografou Campus, 15780, Athens, Greece, email: edrakaki@central.ntua.gr,

Ioannis Sianoudis[2].
2. Department of Physics Chemistry & Material Sciences,
Technological Educational Institute (T.E.I.) of Athens, Ag. Spyridonos, 12210,
Athens, Greece, e-mail: jansian@teiath.gr,

ABSTRACT

In this work we present a technique for examining human skin, based on the *in vivo* measurement of diffuse reflectance spectra in the visible and near-infrared ranges of the electromagnetic spectrum for non-invasive characterisation of haemoglobin oxygenation and pigmentation in skin. Spectra were measured by means of a fiber optic probe, and they were analyzed using an analytical model, based on the Kubelka–Munk theory of scattering and absorption within inhomogeneous materials. To evaluate the utility of the model, skin sites with variable melanin content were studied on individuals with different skin types or with pathological skin conditions. The results of the analysis indicated that it is possible to obtain quantitative information about main skin pigments, as well as basic information regarding the scattering properties of the skin. In addition to quantification of haemoglobin and melanin, qualitative information on the redox state of the blood may also be obtained. The proposed analytical model could be a helpful tool to monitor and evaluate the variations in the biological skin tissue data and its medical conditions.

Keywords: Reflectance model, hemoglobin, melanin, optical properties, reflectance, scattering, absorbance, hemoglobin oxygenation

INTRODUCTION

A. THEORETICAL CONSIDERATIONS

The basis of spectrophotometry is Lambert–Beer's law, where the total light absorption from a solution with more than one substance equals the sum of absorption from each of the substances, and is proportional to the light path. This applies to light transmission in a solution with no scattering, and a known light path. However, reflectance spectrophotometry in tissues is based on scattering and the light path is unknown. Twersky (1962, 1970a, 1970b) originally formulated the basic theory of light scattering in tissues, which is quite complicated for practical use. Essentially, it divides the optical properties of tissues into an absorbing compound due to the substance to be measured, and a scattering compound due to the media (Pittman and Duling 1975a, Steinke and Shepherd 1986). Simplifying, the optical density (OD) of tissues can be expressed as (Zourabian A *et al* 2000, Leung TS *et al* 2006).

$$\mathrm{OD}=\sum_i \varepsilon_i C_i L B + G \qquad (1)$$

όπου B is a compound scatter factor, which depends on wavelength, haematocrit, optical path length and properties of the scattering media such as particle concentration, size, shape and orientation,G is a geometrical measurements factor, L is the distance between detector and light source (here 400 μm), ενώ i is the chomophore, ε_i is the molar extinction coefficient for chromophores at λ.
Optical density can represent the attenuation of light into a tissue, and from many authors can be expressed with the negative logarithm of tissue reflectance (Delpy DT et al 1988, Jacques SL *et al* 1997, Kim JG *et al* 2005, Drakaki E, *et al* 2006).
If we have any change in any chromophore I (e.g. hemoglobin, water, melanin, birilubin, β-carotene), a spectral change in the measured reflectance can occur. Then, while the ε_i and L remain constant, the

factors *B* and *G* are assumed to be constant. We therefore find that the change in optical density (Eq.1) is given by the equation (2) (Zourabian A *et al* 2000):

$$\Delta OD\ (\lambda) = -\ \mathrm{Log}(R_{\tau\varepsilon\lambda}/R_{\alpha\rho\chi}) = \sum_i \varepsilon_i * (\Delta C_i) * L * B \Rightarrow$$

$$\Delta OD\ (\lambda) = \left(\varepsilon_{HbO_2}(\lambda)\Delta[C_{HbO_2}] + \varepsilon_{Hb}(\lambda)\Delta[C_{Hb}]\right) L * B(\lambda) \qquad (2)$$

From the equation (2) we could evaluate relatively the change in the concentration of oxy-hemoglobin.

The oxygen saturation is defined by the ratio between oxy-haemoglobin and total haemoglobin. The oxygen saturation SpO2 is generally defined by the ratio between densities of oxy-haemoglobin and total haemoglobin as follows:

$$SpO_2 = \frac{C_{HbO_2}}{C_{Hb} + C_{HbO_2}} \qquad (3)$$

where C_{HbO2} and C_{Hb} indicate the concentrations of deoxy-hemoglobin and oxyhemoglobin respectively (Zonios G *et al* 2001). The equation (3) about the haemoglobin saturation in oxygen is often expressed as ratio per cent as follows:

$$SpO_2\,\% = \frac{C_{HbO_2}}{C_{Hb} + C_{HbO_2}}\,\% \qquad (4)$$

The oxygen saturation 0.97 ~ 0.98 is normal in the arterial blood, about 0.70 is normal in venous blood.

By taking the ratio K of the changes in optical density measured at two different wavelengths (Eq.2) we get the following expression:

$$K = \frac{\Delta OD(\lambda_1)}{\Delta OD(\lambda_2)} = \frac{\left(\varepsilon_{HbO_2}(\lambda_1)SpO_2 + \varepsilon_{Hb}(\lambda_1)(1 - SpO_2)\right)\Delta[C_{Hb_{\text{ολικο}}}]L * B(\lambda_1)}{\left(\varepsilon_{HbO_2}(\lambda_2)SpO_2 + \varepsilon_{Hb}(\lambda_2)(1 - SpO_2)\right)\Delta[C_{Hb_{\text{ολικο}}}]L * B(\lambda_2)} \qquad (5)$$

By solving for haemoglobin oxygen saturation SpO2 we obtain the following final expression:

$$SpO_2 = \frac{\varepsilon_{Hb}(\lambda_2)K * \left(\frac{B(\lambda_2)}{B(\lambda_1)}\right) - \varepsilon_{Hb}(\lambda_1)}{\left(\varepsilon_{HbO_2}(\lambda_1) - \varepsilon_{Hb}(\lambda_1)\right) - K * \left(\frac{B(\lambda_2)}{B(\lambda_1)}\right) * \left(\varepsilon_{HbO_2}(\lambda_2) - \varepsilon_{Hb}(\lambda_2)\right)} \qquad (6)$$

The *B* factor can be estimated by solving the photon diffusion equation (Schmitt J M 1991, Marble DR, *et al* 1994, Haskell RC *et al* 1994) for the appropriate measurement geometry (Zourabian A *et al* 2000).

We could, during the variation of oxygenation of hemoglobin, find the concentration of oxy-hemoglobin from the equation (2), after some mathematical operations.

$$\Delta[C_{HbO_2}] = \frac{\varepsilon_{Hb}(\lambda_2)\Delta[OD(\lambda_1)] - \varepsilon_{Hb}(\lambda_1)\Delta[OD(\lambda_2)]}{L(\varepsilon_{Hb}(\lambda_2)\varepsilon_{HbO_2}(\lambda_1) - \varepsilon_{Hb}(\lambda_2)\varepsilon_{HbO_2}(\lambda_2))} \qquad (7)$$

B. SKIN REFLECTANCE MODEL

We calculated a theoretical model of skin reflectance model, taking into account the different optical behavior, due to different color, sex, chromophore concentration or skin healthy condition.
For this research, we relied on previous research that Poirier G 2003, Takanori Igarashi *et al* 2005, Doi M *et al* 2003, Cerussi AE 1999, Störring Moritz 2004 had been done.

This skin model contains set of the different skin layers with varied chromophore concentration and skin layer thickness at papillary dermis, at *superficial horizontial plexus* and at *Reticular Dermis*, The basic scheme is shown at figure 1.

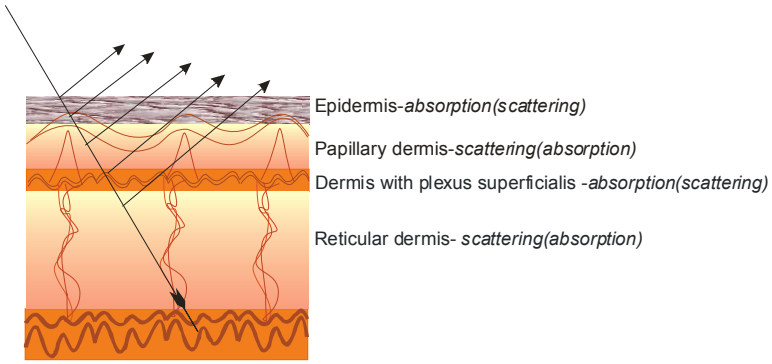

Figure 1. Schematic design of skin tissue

The model is based on the Kubelka Munk (KM) theory (Kubelka P et *al* 1931, Kubelka P 1948, Kubelka P 1954, Ishimaru A 1978-p.191, Doi M *et al* 2003, Shakespeare T *et al* 2004, Störring M 2004, Takanori Igarashi *etal* 2005). For one skin layer the reflectance and transmittance coefficient are given from the equation of the KM theory:

$$R(\lambda) = \frac{(1-\beta^2)(e^{Kd} - e^{-Kd})}{(1+\beta)^2 e^{Kd} - (1-\beta)^2 e^{-Kd}} \quad (1)$$

$$T(\lambda) = \frac{4\beta}{(1+\beta)^2 e^{Kd} - (1-\beta)^2 e^{-Kd}} \quad (2)$$

where $K = \sqrt{\mu_\alpha(\mu_\alpha + \mu_s)}$, $\beta = \sqrt{\frac{\mu_\alpha}{\mu_\alpha + \mu_s}}$, μ_α and μ_s are resulted from Lambert- Beer's law, Mie-Rayleigh theory respectively.
If we had two skin layers of known reflectivity and transmittance R_1, R_2, T_1 and T_2, according all he possible optical interactions we have an infinitive sum (figure 2).

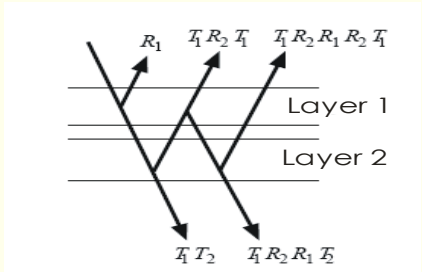

Figure 2. Optical interactions representation between two tissue layers

$$R_{12}=R_1+T_1R_2T_1+T_1R_2R_1R_2T_1+\ldots \quad (3)$$
$$T_{12}=T_1T_2+T_2R_1R_2T_1+\ldots \quad (4)$$

which could be simplified into $R_{12} = R_1 + \frac{T_1^2 R_2}{1 - R_1 R_2}$ and $T_{12} = \frac{T_1 T_2}{1 - R_1 R_2}$

Thus, reflectance and transmittance for n layers could be calculate accordingly (Claridge E *etal* 2003, Störring Moritz 2004, Takanori Igarashi *et al* 2005, Doi M *et al* 2003)

$$R_{12\ldots n} = R_{1\ldots n-1} + \frac{T_{12..n-1}^2 R_n}{1 - R_{12..n-1} R_n} \quad (5)$$

and

$$T_{12...n} = \frac{T_{12..n} - 1T_n}{1 - R_{12..n-1}R_n} \quad (6)$$

After further analysis for four skin layers from the above equations, we have:

$$R_{1234} = R_{123} + \frac{T_{123}^2 R_4}{1 - R_{123}R_4} \quad (7)$$

and

$$T_{1234} = \frac{T_{123\backslash}T_4}{1 - R_{12..n-1}R_n} \quad (8)$$

METHODOLOGY AND SAMPLE

A. EXPERIMENTAL SET-UP

Reflectance measurements were performed with skin illumination by a tungsten halogen source (HL-2000, Avantes). The excitation light was transmitted into bifurcated fiber optics bundle (QR200-7-UV/VIS-BX, Ocean Optics and FCB-UV400-2, Avantes), which also helped to collect the diffuse reflectance spectra from the experimented skin area. The reflectance spectra were then detected as a function of time, before, during, and after occlusion and analyzed by a spectrometer (Model S2000 and HR2000, Ocean Optics) and the software OOIIrrad-C and OOIBase32 (Ocean Optics). The experimental set up is shown in figure 3.

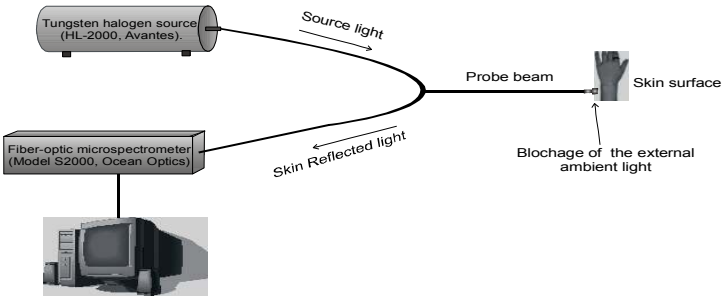

Figure 3. Experimental setup for diffuse reflectance measurements of skin samples.

B. HUMAN SKIN SAMPLES

Several volunteers from our undergraduate laboratories were supposed to diffused reflectance spectroscopy of their skin. Five to seven points from several hand places were examined for each volunteer, according to the anatomic area, the oxygenation condition and the skin phototype. The skin phototypes were defined according to the classifications that based on Fitzpatrick's sun-reactive skin types.

RESULTS AND DISCUSSION

A. PIGMENTATION

Increased concentration in melanin enhances the absorption of human skin tissue. According the Beer – Lambert law the **optical density OD** is related to the diffuse reflectance spectra with the equation below: OD= - Log [Rd] and connect absorbance of skin pigmentation with the growth of melanocytes (Figs. 4, 5).

Quantification of melanin pigment could be determined by the **Melanin index *M***, with the equation ***M***= κ ·(ODλ1-ODλ2)/(λ1-λ2) , where k calibration coefficient, ODλ1 και ODλ2 the optical densities at λ1 and λ2 respectively. We choose λ1:365 nm and λ2:395 nm, because of the high melanin absorbance. From the figure 6 we can see the linear dependence of **Melanin Index *M***, with the estimated percentage of melanin at the skin tissue under investigation (Fig. 6).

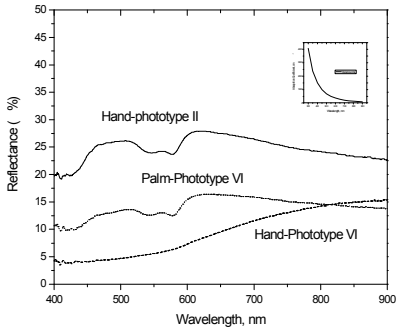

Figure 4. Diffuse reflectance spectra by two different prototypes. In the insert graph, the melanin absorbance spectrum.

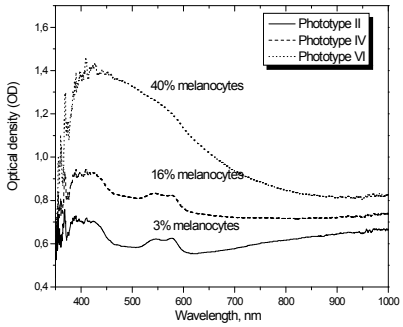

Figure 5. Optical density spectra by three different skin phototypes.

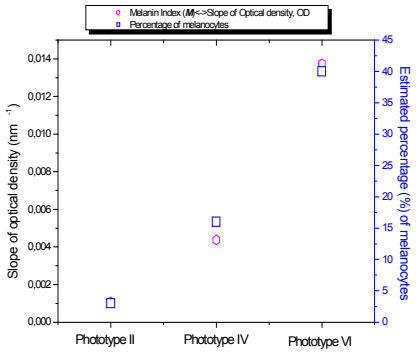

Figure 6. Gradient of optical density of different prototypes versus percentage of melanocytes.

B. OXYGENATION

The first large absorption spectral area of 100% oxyhemoglobin (Soret band) appears at 415 nm and secondary spectral areas at ~542 nm and ~577 nm. The non oxygenated haemoglobin absorption spectra is totally different, with the Soret band being red at 431 nm, with the bands α and β grouped at 555 nm and a secondary absorption peak at 760 nm. The absorption of non-oxygenated haemoglobin is higher at 640 nm and 670 nm, while oxygenated haemoglobin appears to absorb less after 620 nm. It is known that the absorption of hemoglobin is related to its saturation with the oxygen.

During hypoxia the peaks of 542 nm and 577 nm are being disappeared (characteristic absorption peaks of oxygenated hemoglobin), with a overall decrease of the reflectance intensity, especially after λ>600 nm, spectral area of the non oxygenated hemoglobin (Fig. 7). After the effect of hypoxia, there is an intense increase of oxy-hemoglobin and an inverse behavior at non oxygenated hemoglobin (at 80s, 84s και 85s), until both blood components *return* to their physiological levels.

At figure 6 from the normalized reflectance spectra versus wavelength we can see clearly the transition from oxy-hemoglobin to non-oxygenated hemoglobin at their characteristic spectral absorption peaks (Sianoudis JA *et al* 2005).

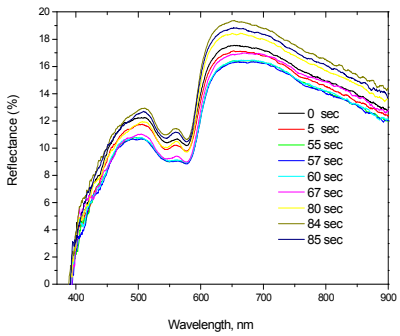

Figure 7. Skin Reflectance (%) versus time before (t=0 s),during (at 55s, 57s, 60s and 67s) and after hypoxia (at 80s, 84s και 85s), with relaxation of the incident pressure.

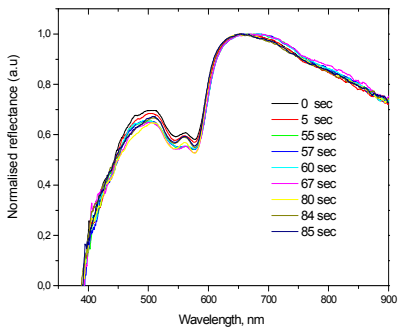

Figure 8. Normalized skin Reflectance (%) versus time before (t=0 s),during (at 55s, 57s, 60s and 67s) and after hypoxia (at 80s, 84s και 85s), with relaxation of the incident pressure.

The rate of change and other biological remarks can not been discriminate at the figs.7, 8 and for that reason the ratio of optical density at λ1: 544 nm to λ2: 560 nm versus the ratio of optical density at λ3: 577 nm to λ4: 586 nm at fig. 9, help us to resolve oxygenated and not oxygenated skin tissue conditions. Those spectral points were chosen accordingly, since Hb_{O2}, and Hb exhibit equal absorption values. From the figure 9 we can notice that the non-oxygenated skin tissues can be grouped (exp. points at the up right corner, with the sign "**no**"), from the rest skin tissues, where the concentration of oxy-hemoglobin is in physiological levels (exp. points with the sign "**o**"). This spectral characteristic can be used for the modeling pathological tissue conditions, where the oxygen saturation is one of their indications (e.g. cancerous skin tissues).

The choices of the appropriate wavelengths under investigation were those where there is no melanin, hemoglobin and water absorption. At the figure 10 we can see the normalized gradient of oxygen at λ1= 675 nm and λ2=700 nm versus time before (t=0 s), during (at 55s, 57s, 60s and 67s) and after hypoxia (at 80s, 84s και 85s), with relaxation of the incident pressure.

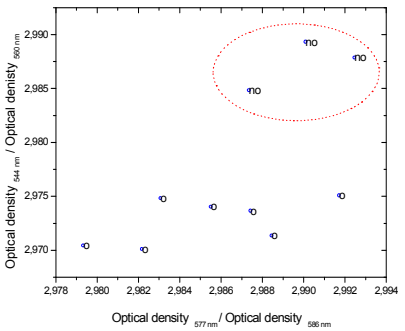

Figure 9. Ratio of optical density at λ1: 544nm to λ2: 560 nm versus the ratio of optical density at λ3: 577 nm to λ4: 586 nm, for discrimination of oxygenated and not oxygenated skin tissue conditions.

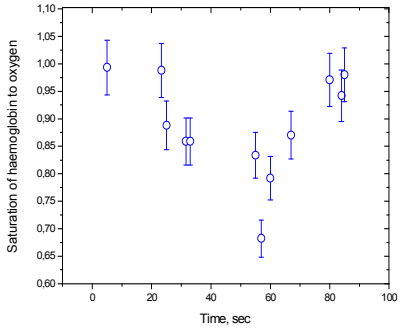

Figure 10. Normalized gradient of oxygen versus time before (t=0 s),during (at 55s, 57s, 60s and 67s) and after hypoxia (at 80s, 84s και 85s), with relaxation of the incident pressure.

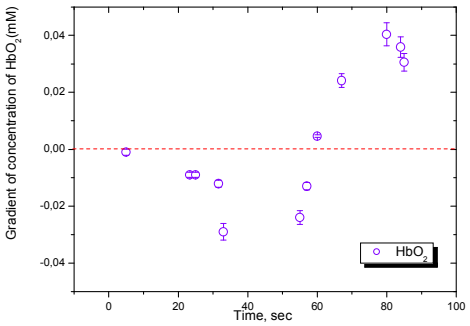

Figure 11. Gradient of oxygenated hemoglobin versus time before (t=0 s),during (at 55s, 57s, 60s and 67s) and after hypoxia (at 80s, 84s και 85s), with relaxation of the incident pressure.

At the figure 10 the change in oxygen saturation during the experiment of occlusion is shown, while at the figure 5b the change of concentration of oxygenated hemoglobin can be seen. We can notice the slow transition of the oxygenated hemoglobin to the deoxy-hemoglobin, when after the release of the occlusion; a faster transition is occurred, with a trend to return to physiological levels. At the figure 11 we can see the slower change rate of concentration of oxygenated hemoglobin, due the remained small percent of that kind of hemoglobin during the occlusion.

At the figure 12, we have various concentrations of melanin from 1% to 20%. We noticed a reduction of the reflectance intensity, especially at the lower wavelengths and almost erasure of the spectral characteristics of oxygenated hemoglobin, as we similarly noticed at the experimental results at figure 4. At the figure 13, we have varied the thickness of epidermis from 10 μm till 200 μm, and we noticed an attenuation of the total reflectance intensity, since more of the incident irradiation is being absorbed form the melanin. Furthermore less irradiation is reaching the dermis with plexus superificialis net, and the characteristic spectral pattern W of oxygenated hemoglobin is being less discernible for thicker layers of epidermis.

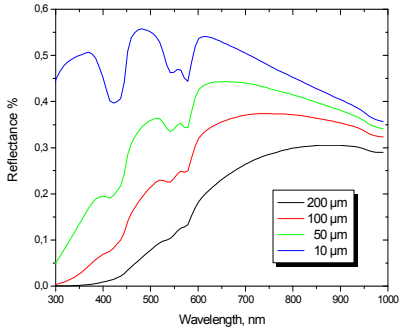

Figure 12. Reflectance of skin tissue at various melanin concentrations.

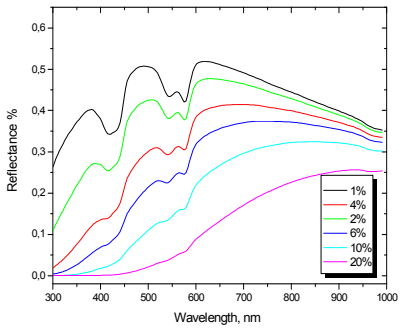

Figure 13. Reflectance of skin tissue with 6% melanin concentration at various epidermis thickness (10μm-200μm).

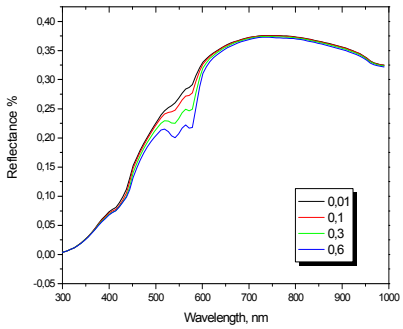

Figure 14. .Reflectance of skin tissue with 6% melanin concentration at various hemoglobin concentrations (cHb =0.01-…-0.6) at the dermis-plexus superficialis layer.

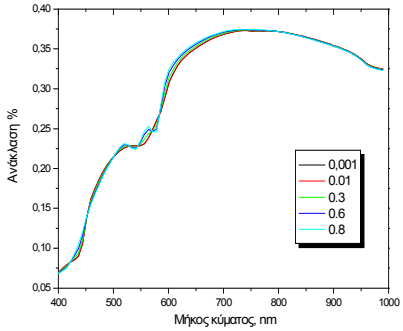

Figure 16. Reflectance of skin tissue with 6% melanin concentration at various oxygen concentrations at the dermis-plexus superficialis layer.

At the figure 14, we increased the percentage of the hemoglobin into the blood (f =0.01-…-0.6) at the plexus superficialis net layer at dermis. We noticed a reduction of reflectance at eh spectral area 450 nm -550 nm, with the characteristic pattern W, to be more profound and giving to the skin a reddish appearance. At the figure 15 various concentration of oxygen O into blood (O =0.001-…-0.8) at the plexus superficialis net layer at dermis introduced a slight variation at the reflectance spectra, with more intense absence of the W spectral characteristic of hemoglobin at the spectra area near 550 nm. At the figure 16 we have variation of the thickness of the reticular dermis from 900 μm till 2000 μm. We noticed an increase in reflectance intensity, especially at the longer wavelengths, due to the Mie scattering.

Comparing experimental and theoretical results we observed similar spectral and optical behavior (fig. 17). Nevertheless, there are some slight declinations, due to the uncertainty and the variability of the melanin and hemoglobin concentration in our experiments and due to the influence of the spectral dependence of the lamp irradiation that was used for the diffuse reflectance experiments.

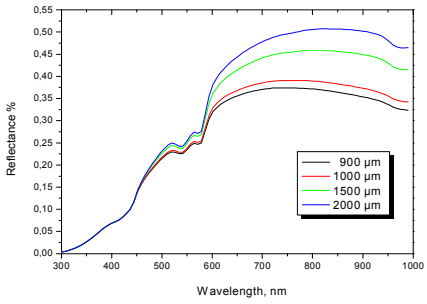

Figure 16. Reflectance of skin tissue with 6% melanin concentration at various thicknesses of reticular dermis (900 μm-2000 μm).

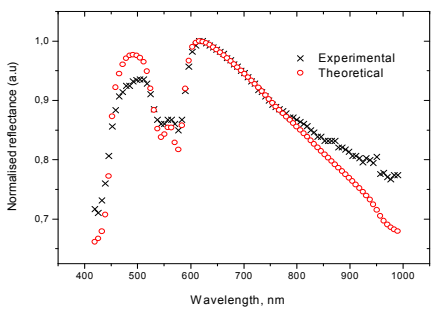

Figure 17. Comparison of simulated reflectance spectra with 4% melanin concentration with a measured reflectance spectra of a light skin person.

CONCLUSION

In this work we presented a technique for examining human skin, based on the *in vivo* measurement of diffuse reflectance spectra in the visible and near-infrared ranges of the electromagnetic spectrum for non-invasive characterisation of haemoglobin oxygenation and pigmentation in skin.

In our research we studied the influence of chromophores inside skin samples at the reflectance spectra. The inhomogeneous distribution and the different concentration of melanin and oxygenated and non - oxygenated hemoglobin were being related qualitative and quantitative with the diffuse reflectance spectra.

A theoretical model of diffuse reflectance spectra was developed thought spectroscopic data and the help of Kubelka Munk theory.That proposed analytical model could be a helpful tool to monitor and evaluate the variations in the biological skin tissue data and its medical conditions.

A big number of biomedical applications in diagnosis of pathological skin tissue with direct and non-invansive analysis (e.g. hypermelanosis, malignant tumors, hemangiamas, hematomas, skin inflammations etc) can be advanced and benefit. However as far as concern the big skin case variation more statistical study and interpretation must to be made.

ACKNOWLEDGMENTS

This work was supported by TEI of Athens, research program “Athena 2004”.
This work was presented at the Annual Meeting of the Deutsche Physikalische Gesellschaft and DPG - spring meeting of the Division Condensed Matter-Medizinphysik, (71th Jahrestagung der Deutschen Physikalischen Gesellschaft und DPG Frühjahrstagung des Arbeitskreises Festkörperphysik Frühjahrstagung), as a Poster at Regensburg 2007 (March 27 – 29, 2007), Germany.

REFERENCES

Cerussi Albert Edward (1999) PhD thesis: Quantitative frequency–domain fluorescence spectroscopy in tissues and tissue like media. Rensselaer Polytechnic Institute, University of Illinois, Urbana-Champaign, USA

Claridge E, Cotton S, Hall P, Moncrieff M (2003) From colour to tissue histology: Physics-based interpretation of images of pigmented skin lesions. Medical Image Analysis 7: 489–502

Delpy DT, Cope M, van der Zee P, Arridge S, Wrayt S, Wyatt J (1988) Estimation of optical pathlength through tissue from direct time of flight measurement. Phys Med Biol 33:1433-1442

Doi M, Tominaga S (2003) Spectral estimation of human skin color using the Kubelka-Munk theory. Proc SPIE 5008:221-228

Drakaki E, Makropoulou M, Serafetinides A, Borisova E, Avramov L, Sianoudis JA (2006) Optical spectroscopic studies of animal skin used in modelling of human cutaneous tissue. Proc SPIE Vol. 6604, 14th International School on Quantum Electronics: Laser Physics and Applications, Peter A. Atanasov; Tanja N. Dreischuh; Sanka V. Gateva; Lubomir M. Kovachev, Editors, 66042K, 18 − 22 September 2006, Sunny Beach, Bulgaria, DOI: 10.1117/12.727723

Jacques SL, Saidi I, Ladner A, Oelberg D (1997) Developing an optical fiber reflectance spectrometer to monitor bilirubinemia in neonates SPIE Proceedings:Laser-Tissue Interactions 2975:115-124

Haskell RC, Svaasand LO, Tsay T, Feng T, McAdams MS, Tromberg BJ (1994) Boundary conditions for the diffusion equation in radiative transfer. J. Opt. Soc. Am. A 11: 2727–2741

Ishimaru A (1978) Wave Propagation and Scattering in Random Media, Volume I. New York: Academic.

Kim JG, Xia M, Liu H (2005) Extinction coefficients of hemoglobin for near-infrared spectroscopy of tissue. IEEE Engin Med Biol Magasine: Engineering in Genomics. 118-121

Kubelka P (1948). New contributions to the optics of intensely light-scattering materials, part i. Journal of the Optical Society of America, 38:448–457

Kubelka P, F. Munk. (1931) Ein beitrag zur optik der farbanstriche (translation by Steve Westin available at http://graphics.cornell.edu/_westin/pubs/kubelka.pdf). Z. Tech. Physik., 12:593,

Kubelka P (1954) New contributions to the optics of intensely light-scattering materials, part ii: Nonhomogeneous layers. Journal of the Optical Society of America, 44:330–335

Leung TS, Tachtsidis I, Smith M, Delpy DT, Elwell CE (2006) Measurement of the absolute optical properties and cerebral blood volume of the adult human head with hybrid differential and spatially resolved spectroscopy. Phys Med Biol 51:703–717

Marble DR, Burns DH, Cheung PW (1994) Diffusion-based model for pulse oximetry: In-vivo and in-vitro comparisons. Appl Opt 33: 1279–1285 (cited by Zourabian A et al 2000)

Poirier Guillaume (2003) Human Skin Modelling and Rendering, PhD thesis, University of Waterloo, Waterloo, Ontario, Canada

Pittman R and Duling B 1975a A new method for the measurement of percent oxyhemoglobin J. Appl. Physiol. 38 315–20

Schmitt JM (1991) Simple photon diffusion analysis of the effects of multiple scattering on pulse oximetry IEEE Trans Biomed Eng 38: 1194–1203 (cited by Zourabian A et al 2000)

Shakespeare T, Shakespeare J (2002) A Fluorescent Extension to the Kubelka–Munk Model, COLOR research and application, 4-14

Sianoudis JA., Drakaki E, Valais J (2005) Measurements on skin tissue with the spectroscopic method of Diffuse Reflectance: A first preliminary approach. E-Journal of Science & Technology (e-JST), 1:43-57

Steinke J M and Shepherd A P 1986 Role of light scattering in whole blood oximetry IEEE. Trans. Biomed. Eng. 33 294–301

Störring Moritz (2004) Computer Vision and Human Skin Colour, Ph.D. Dissertation, Computer Vision & Media Technology Laboratory, Faculty of Engineering and Science, Aalborg University, Denmark

Takanori Igarashi, Ko Nishino, Shree K. Nayar (2005) The Appearance of Human Skin Technical Report: CUCS-024-05, Department of Computer Science, Columbia University New York, NY 10027, USA

Twersky V 1962 Multiple scattering of waves and optical phenomina J. Opt. Soc. Am. 52 145–71

Twersky V 1970a Absorption and multiple scattering by biological suspensions J. Opt. Soc. Am. 60 1084–93

Twersky V 1970b Interface effects in multiple scattering by large, low-refracting absorbing particles J. Opt. Soc. Am. 60 908–14

Zonios G, Bykowski J, Kollias N (2001) Skin melanin, hemoglobin, and light scattering properties can be quantitatively assessed In vivo using diffuse reflectance spectroscopy. J Invest Dermatol. 117:1452-1457

Zourabian A, Siegel A, Chance B, Ramanujan N, Rode M, Boas DA (2000) Trans-abdominal monitoring of fetal arterial blood oxygenation using pulse oximetry. J. Biom. Opt. 5: 391–405